Available online at www.sciencedirect.com
ScienceDirect
Journal of Photochemistry and Photobiology A: Chemistry 194 (2008) 327–332
Journal of Photochemistry and Photobiology A:Chemistry
www.elsevier.com/locate/jphotochem

Synthesis, photoconductivity, and photogeneration efficiency of polysiloxanes bearing hole-conductors for photorefractive materials

In Kyu Moon *, Jin-Woo Oh, Nakjoong Kim

Department of Chemistry, Hanyang University, Seoul 131-791, South Korea

Received 31 May 2007; received in revised form 1 August 2007; accepted 29 August 2007
Available online 1 September 2007

Abstract

Two series of polysiloxanes, namely, PSX-DCZ and PSX-TPD, with hole-transporting moieties have been synthesized and their electronic absorption, electrochemical behavior, quantum efficiency of charge generation, and photoconductivity is also studied. Our results show that the photocurrent were found to be *ca*. 3280 nA for PSX-DCZ/C_{60} and *ca*. 3400 nA for the PSX-TPD/C_{60} at wavelength of 633 nm and an electric field of 60 V/μm. We also obtained the quantum efficiency of charge generation as high as 25.2×10^{-5} for PSX-DCZ/C_{60} and 31.1×10^{-5} for PSX-TPD/C_{60} (at $\lambda = 633$ nm, $E = 60$ V/μm). The photoconductivity of these polymers is found to be greater than that of PVK/C_{60}.

Keywords: 3,3′-Bicarbazole; *N*,*N*′-diphenyl-*N*,*N*′-bis(4-methylphenyl)-[1,1′-biphenyl]-4,4′-diamine; Polysiloxane; Photoconductivity

1. Introduction

Materials based on arylamines, *e.g*., carbazole and triphenylamine derivatives, have been studied extensively due to their interesting physical, photochemical, and electrochemical properties [1,2]. These materials can form stable radical cations without undergoing subsequent chemical transformation. The development of arylamine-based materials for optoelectronic applications has drawn much attention over the last two decades. During this time, there have been significant advances made in this field, leading to the use of organic materials in many present day applications such as hole-transporting materials or emitter for organic light-emitting diodes, xerographic technologies, field-effect transistors, solar cells, and photorefractive materials [4–7]. Especially, arylamine or carbazole-based polymers have been investigated extensively due to their good hole transport and photorefractivity.

The photorefractive effect refers to the spatial modulation of the refractive index of a material due to the light-induced redistribution of the electronic charge. The main characteristics governing the photorefractive are the electro-optical activity and the photoconductivity of a material [7]. Among the photorefractivity factors, the photoconductivity is governed by the photogeneration and the transport of charges. The majority of photorefractive polymer composites reported so far are based on the photoconductor poly(*N*-vinylcarbazole) (PVK). Nevertheless, PVK-based photorefractive devices still have drawbacks, especially the extreme brittleness of the material. These properties lead to the formation of electro-optic chromophore aggregates on heating during device formation or operation.

To solve this problem, we applied the polysiloxane-backbone containing the hole-transporting moiety. Polysiloxane has a very low glass transition temperature. And also, to improve photoconductivity of photoconductor, the replacement of the carbazole with 3,3′-dicarbazole (DCZ) or *N*,*N*′-diphenyl-*N*,*N*′-bis(3-methylphenyl)-[1,1′-biphenyl]-4,4′-diamine (TPD) unit leads to new hole-transporting polymers [9,10]. This approach makes it possible to realize highly efficient PHOTOREFRACTIVITY without an excess of plasticizers, and can speed up the formation of the photorefractive grating.

In these respects, the development of new hole-transporting polymers is greatly needed for commercialization. This paper deals with the synthesis of two polysiloxanes with hole-transporting moieties, DCZ and TPD by a platinum-catalyzed hydrosiliation method. Moreover, we also discuss improved photoconductivity with the hole-transporting units by doping with C_{60}.

* Corresponding author. Tel.: +82 2 2220 0935; fax: +82 2 2295 0572.
E-mail address: inkmoon@naver.com (I.K. Moon).

1010-6030/$ – see front matter © 2007 Elsevier B.V. All rights reserved.
doi:10.1016/j.jphotochem.2007.08.031

2. Experimental

2.1. Materials and instrumentation

All reagents and solvents were used as received from Aldrich Chemical Company. The solvents were dried using standard procedures. PVK and C_{60} were purchased from Aldrich Chemical Company. The chemical structure of the new multifunctional molecule was characterized by ^{1}H NMR spectrometry (Varian, INOVA, 400 MHz) and FT-IR spectrometry (Perkin-Elmer, Paragon 500). The absorption maximum (λ_{max}) of molecule in methylene chloride solution was recorded in Duksan Mechasys, Optizen III. New polymers were synthesized using the reaction scheme, as shown in Scheme 1. The glass transition temperature (T_g) of this composite determined by differential scanning calorimetry (DSC, Perkin-Elmer DSC7). The molecular weight and polydispersity were determined in THF solvent by a Waters GPC-410 calibrated with polystyrene standards.

2.2. Sample preparation and measurement

The photogeneration efficiency of these polymers were evaluated using the standard photoinduced discharge technique, which is the basis of the xerographic process in the photocopying systems. Polymer mixture (PSX-DCZ:C_{60} = 69:1 and PSX-TPD:C_{60} = 69:1 wt%) are dissolved in a 1,1,2,2-tetrachloroethane (TCE) mixture and the layers are fabricated by doctor-blade technique on a 2.5 cm × 2.5 cm indium–tin-oxide (ITO) glass substrate. Layer thickness (in the 3.5 μm range) is measured by Metricon. Xerographic discharge experiments were performed with a wavelength of 633 nm (I = 3.6 mW/cm^2) The quantum yield was calculated from the measured photodecays taking into account corrections for the light source performance, spectral characteristic of the optical path and absorption by the active area of the sample.

The devices (sandwich geometry ITO/polymer(C_{60})/Al) for the measuring photoconductivity by the simple DC photocurrent method were prepared by evaporating Al on pre-coated polymers in vacuum. The top contact was semitransparent Al. The photoconductivity measurements by the simple DC photocurrent method were determined at the wavelength of 633 nm using a I = 0.31 mW/cm^2. All experiments were carried out under ambient conditions and room temperature.

2.3. Synthesis

2.3.1. N,N′-(2,2′-ethylhexyl)-3,3′-bicarbazyl (DCZ)

To a stirred solution of *N*-(2-ethylhexyl)carbazole (1 equiv.) in 70 ml dry chloroform under nitrogen atmosphere was cooled to 0 °C. $FeCl_3$ (4 equiv.) was added to the mixture. After stirring at room temperature during 4 h, 150 ml water was added. The organic layer was separated, dried over $MgSO_4$, filtered and concentrated. The mixture was purified by column chromatography (SiO_2, hexane/ethyl acetate = 98/2). Yield = 89% (colorless oil, ^{1}H NMR ($CDCl_3$, ppm) δ 0.94 (m, 12H), 1.40 (m, 16H), 2.11 (m, 2H), 4.23 (m, 4H), 7. 10–8.52 (m, 14H).

2.3.2. N,N′-di(2-ethylhexyl)-3,3′-bicarbazyle-6-carbaldehyde (DCZ-CHO)

1.3 Equiv. freshly distilled phosphorus oxychloride was slowly added to DMF (1.5 equiv.) at a temperature between 0 and 5 °C. After additional stirring for 1 h at room temperature, this solution was added to a stirred solution of **DCZ** (1 equiv.) in 20 ml of 1,2-dichloroethane. This reaction mixture was stirred for another hour at 60 °C and then allowed to cool down to room temperature. Hereafter the mixture was poured into a solution of 10 g sodium acetate in 100 ml water; this mixture was extracted three times with dichloromethane. The combined organic layers were washed twice with water, and dried over $MgSO_4$. The mixture was purified by column chromatography (SiO_2, hexane/dichloromethane = 75/25). Yield = 58% (yellow oil). ^{1}H NMR ($CDCl_3$, ppm) δ 0.94 (m, 12H), 1.40 (m, 16H), 2.11 (m, 2H), 4.23 (m, 4H), 7.26 (m, 1H), 7.52–7.40 (m, 5H), 7.81 (d, 1H), 7.89 (d, 1H), 8.02 (d, 1H), 8.17 (d, 1H), 8.39 (d, 1H), 8.46 (d, 1H), 8.68 (d, 1H), 10.09 (s, 1H).

2.3.3. N,N′-di(2-ethylhexyl)-6-hydroxy-3,3′-bicarbazyl (DCZ-OH)

To a **DCZ-CHO** (1 equiv.) in 75 ml abs. MeOH in a nitrogen atmosphere was added 2 ml hydrogen peroxide (35% in

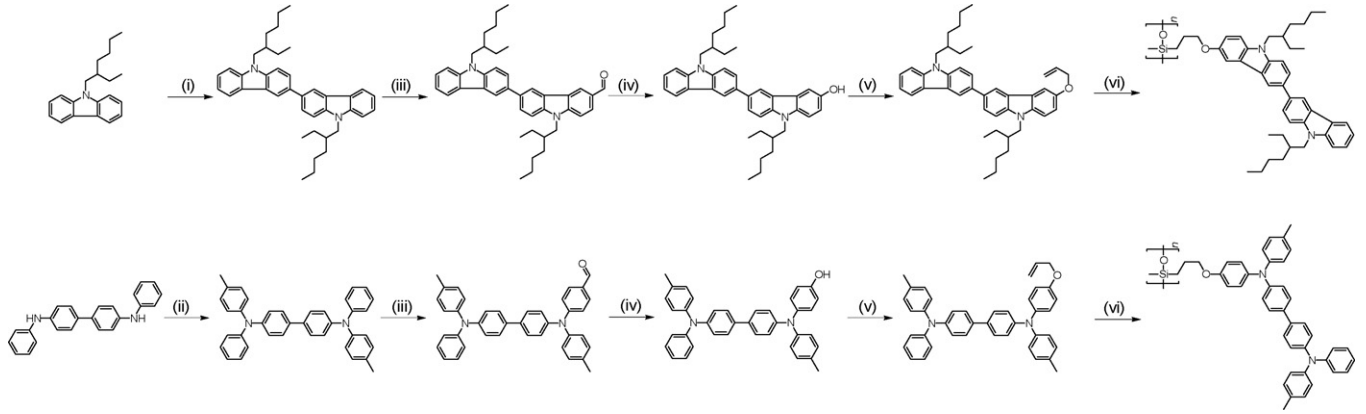

Scheme 1. Synthetic route of the monomers and the polymers. *Reaction conditions*: (i) $FeCl_3$/methylene chloride; (ii) Cu/4-iodotoluene/K_2CO_3/docecane; (iii) $POCl_3$/DMF/dichloroethane; (iv) H_2O_2/H_2SO_4/MeOH; (v) allyl bromide/KOH/DMF; (vi) poly(methylhydro)siloxane/hexachloroplatinate(IV) hydrate/toluene.

water) and 0.1 ml concentrated sulphuric acid. After 2 h stirring at room temperature, the result solution was diluted with 250 ml water and the product extracted with ethyl acetate. The organic layer was washed twice with 200 ml water and after drying evaporated to afford a crude product. The mixture was purified by column chromatography (SiO_2, hexane/ethyl acetate = 7/3). Yield = 87%. ^{1}H NMR ($CDCl_3$, ppm) δ 0.94 (m, 12H), 1.41 (m, 16H), 2.11 (m, 2H), 4.20 (m, 4H), 5.02 (br s, 1H), 7.21–8.41 (m, 13H). IR (KBr pellet, cm^{-1}): 3610 (–OH, str.).

2.3.4. N,N′-di(2-ethylhexyl)-6-allyloxy-3,3′-bicarbazyl (DCZ-Allyl)

A solution of DCZ-OH (1 equiv.) in dried DMF (50 ml) was treated with a powdered KOH (1.8 equiv.) at room temperature. After stirring for 5 h, allyl bromide (1.1 equiv.) was slowly added. The mixture was stirred at 0 °C for 1 h, and then at 70 °C for 12 h. The resulting solution was poured water. The mixture was extracted with ethyl acetate. The extract was dried with $MgSO_4$ and the solvent was removed at reduced pressure. The mixture was purified by column chromatography (SiO_2, hexane/ethyl acetate = 95/5). Yield = 71%. ^{1}H NMR ($CDCl_3$, ppm) δ 0.94 (m, 12H), 1.41 (m, 16H), 2.11 (m, 2H), 4.20 (m, 4H), 4.62 (d, 2H), 5.23–5.41 (q, 2H), 6.17 (m, 1H), 7.18–8.39 (m, 13H).

2.3.5. N,N′-diphenyl-N,N′-bis(4-methylphenyl)-[1,1′-biphenyl]-4,4′-diamine (TPD)

A solution of *N,N′*-diphenyl-[1,1′-biphenyl]-4,4′-diamine (1 equiv.), 4-iodotoluene (3 equiv.), potassium carbonate (4 equiv.), and copper bronze (8.8 g) in 40 ml docecane was stirred under argon atmosphere at 210 °C for 2 days. After cooling down, the excess iodotoluene was removed together with the solvent by distillation under reduced pressure. The product was extracted by refluxing in 400 ml octane and subsequent hot filtration to remove the inorganic salts. The mixture was purified by column chromatography (SiO_2, hexane/toluene = 3/7). Yield = 78% (white solid). ^{1}H NMR ($CDCl_3$, ppm) δ 2.33 (s, 6H), 6.99–7.44 (m, 26H).

2.3.6. N-(4-Formylphenyl)-N′-phenyl-N,N′-bis(4-methylphenyl)-[1,1′-biphenyl]-4,4′-diamine (TPD-CHO)

TPD-CHO was synthesized through the same condition of **DCZ-CHO**. The desired monoformylated product was isolated from this crude product by column chromatography using silica gel and hexane/toluene (1/9) as the eluent, yielding 50% of a yellow solid. ^{1}H NMR ($CDCl_3$, ppm) δ 2.35 (s, 3H), 2.39 (s, 3H), 7.04–7.71 (m, 25H), 9.82 (s, 1H).

2.3.7. N-(4-Hyroxyphenyl)-N′-phenyl-N,N′-bis(4-methylphenyl)-[1,1′-biphenyl]-4,4′-diamine (TPD-OH)

TPD-OH was synthesized through the same condition of **DCZ-OH**. Yield: 86%. ^{1}H NMR ($CDCl_3$, ppm) δ 2.34 (s, 3H), 2.40 (s, 3H), 5.00 (br s, 1H), 7.98–7.68 (m, 25H). IR (KBr pellet, cm^{-1}): 3615 (–OH, str.).

2.3.8. N-(4-Allyloxyphenyl)-N′-phenyl-N,N′-bis(4-methylphenyl)-[1,1′-biphenyl]-4,4′-diamine (TPD-Allyl)

TPD-Allyl was synthesized through the same condition of **DCZ-Allyl**. The desired monoformylated product was isolated from this crude product by column chromatography using silica gel and hexane/toluene (40/60) as the eluent, yielding 50%. ^{1}H NMR ($CDCl_3$, ppm) δ 2.34 (s, 3H), 2.37 (s, 3H), 4.52 (d, 2H), 5.23–5.43 (q, 2H), 6.07 (m, 1H), 6.82–7.43 (m, 25H).

2.4. General polymerization by the hydrosililation

To a 250 ml two-necked round-bottom flask equipped with a condenser, gas inlet, stir bar, and glass stopper under argon was added toluene (50 ml) and poly(methylhydro)siloxane (1 equiv.) and allyl-compound (1.2 equiv.). Catalytic amount of hexachloroplatinate(IV) hydrate in propanol was added to the mixture. The mixture was stirred at elevated temperature (*ca.* 80 °C) using an oil bath. The reaction progress was monitored using IR spectroscopy. After an initial reaction time of 20 h, an aliquot of the neat reaction solution was evaporated on NaCl plates, and the IR spectrum was recorded to follow the disappearance of the Si–H stretch. If the reaction was incomplete, then additional hexachloroplatinate(IV) hydrate (*ca.* 0.5 ml) was added. This cycle was continued at regular time intervals (*ca.* 1 h) until the silicon–hydrogen signal was no longer present in the IR spectrum. Upon completion, the reaction was cooled to room temperature. Then the reaction solution was added dropwise to an excess of methanol (200 ml). The precipitated polymer residue was dissolved in the minimum amount of THF (*ca.* 15 ml) needed to dissolve the crude polymer completely. This THF solution was precipitated again into an excess of methanol (50 ml). The precipitation process was continued until the polymer residue was free of monomers as determined by ^{1}H NMR. Or, the polymers were purified by Soxhlet extraction with methanol for 2 days. Then the polymer was again dissolved in the dry THF (250 ml). This THF solution was filtered through an ion-exchanged resin filter to remove residual catalyst particles and precipitated in hexane and/or methanol. Residual solvent was evaporated under reduced pressure, and then the obtained polymer was dried in a vacuum oven at room temperature for 2 days.

2.4.1. PSX-DCZ

Yield: 73%. T_g = 129 °C. ^{1}H NMR ($CDCl_3$, ppm) δ −0.29–2.60 (br m, 35H), 4.17–4.31 (br s, 4H), 4.50–4.73 (br s, 2H), 6.80–8.52 (br m, 13H).

2.4.2. PSX-TPD

Yield: 75%. T_g = 102 °C. ^{1}H NMR ($CDCl_3$, ppm) δ −0.10–0.30 (br s, 3H), 1.05–1.22 (br s, 2H), 1.70–1.97 (br s, 2H), 2.28–2.41 (br d, 6H), 3.60–3.98 (br s, 2H), 6.60–7.65 (br m, 25H).

3. Results and discussion

Our approach to the synthesis of functionalized polysiloxanes began with the synthesis of photoconductors bearing **DCZ**

Table 1
Polymerization results of the polysiloxanes

Polymer	Yield (%)	M_n[a]	M_w/M_n[a]	T_g (°C)[b]
PSX-DCZ	73	10,340	2.05	129
PSX-TPD	75	8,380	1.81	102

[a] Determined by gel permeation chromatography based on polystyrene standards using THF as an eluent.
[b] Performed under a nitrogen atmosphere at a heating rate of 10 °C/min.

and **TPD**. The synthesis of **DCZ** and **TPD** was accomplished *via* the oxidative dimerization from *N*-(2-ethylhexyl)carbazole using $FeCl_3$ and an Ullman like coupling from *N,N′*-diphenyl-[1,1′-biphenyl]-4,4′-diamine with 4-iodotoluene using copper as outlined in Scheme 1, respectively. **DCZ-CHO** and **TPD-CHO** could be easily formylated by means of the Vilsmeyer reaction, yielding the monoformylated molecules after separation from the disubtituted product. After that, replacement of the formyl group in aromatic aldehyde by a hydroxyl group using of hydrogen peroxide. **DCZ-Allyl** and **TPD-Allyl** were synthesized by reaction of hydroxyl group with allyl bromide using potassium carbonate as a base yield of >80%. Hydrosililation of photoconducting monomers was carried out in freshly dried toluene at 80 °C for 2 days. The solubility of obtained polymers is very good in common organic solvents such as chloroform, tetrahydrofuran (THF), or toluene. In Table 1, the results for the polymerization were summarized.

The proceeding of the hydrosililation was confirmed by disappearance of the signal at 4.8 ppm in the ^{1}H NMR spectrum and the peak at 2108 cm^{-1} of the starting Si–**H** in the IR spectrum. The ^{1}H NMR spectra of polymers exhibited broad resonance peaks typical of polymers. Fig. 1 shows the UV–vis absorption spectra of the two polysiloxanes in the THF solution. As shown in the absorption spectra, the wavelength of maximum absorption (λ_{max}) of **PSX-DCZ** has a strong absorption band at 304 nm (*sh*. 349), while the λ_{max} of **PSX-TPD** absorbs at 304 and 348 nm. The absorption at 304 nm of **PSX-DCZ** and 348 nm of **PSX-TPD** are attributable to the **DCZ** and the **TPD** moiety, respectively.

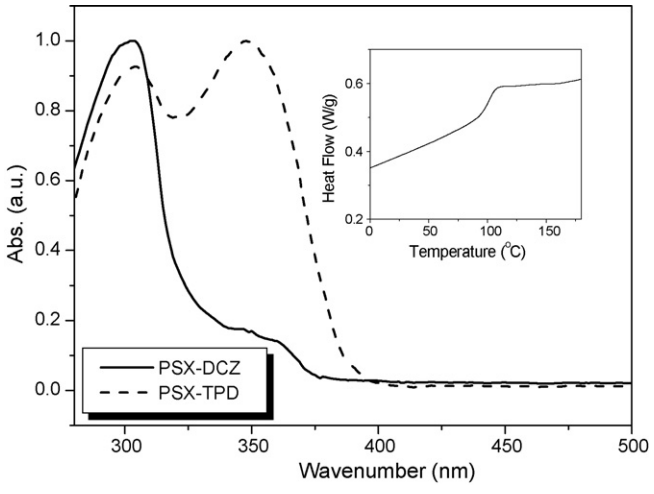

Fig. 1. UV–vis spectra of the PSX-DCZ and the PSX-TPD in THF. The insert figure shows the DSC thermogram of the PSX-TPD.

The electrochemical properties of all polymers were investigated by cyclic voltammetry. The polymers were coated onto a platinum electrode to form a thin film. Then, these were immersed in a 2 mM tetra-*n*-butyl-ammonium tetrafluoroborate acetonitrile solution. The potentials were recorded against an Ag/AgCl as reference electrode and each measurement was using the ferrocence/ferrocenium (Fc) redox system as an internal standard. The energy levels of the polymers were calculated using the ferrocence value of −4.8 eV. The ionization potential (IP) of the **PSX-DCZ** and **PSX-TPD** had −5.87 and −5.49 eV, respectively. It is important to note that there offers among the key to an understanding of space charge field in photorefractive phenomena. The reason for the different photoconductivities for the different charge-transport molecules is a deep connection with the chromophore HOMO. If the HOMO of the chromophore is higher in energy than that of the charge-transport molecule, the chromophore can donate an electron from its HOMO to nearby the charge-transport molecule HOMO. Thus, the chromophore acts as a trap for holes. That is, the depth of the chromophore HOMO as a hole trap can affect the charge mobility, and then turn affects the photoconductivity, with lower photoconductivity for deeper hole traps. The IP level of **PSX-TPD** is 0.38 eV lower than that of **PSX-DCZ**.

Gel permeation chromatography measurements revealed the molecular weight for **PSX-DCZ** (M_w = 21,200, polydispersity index 2.05) and for **PSX-TPD** (M_w = 15,200, polydispersity index 1.81). DSC measurements revealed a glass transition temperature (T_g) of 129 °C for **PSX-DCZ** and 102 °C for **PSX-TPD** (Fig. 1).

The photoconductivity, σ_{ph}, is governed by the photogeneration and the transport of charges and may be written for the case of mobile holes as [10]:

$$\sigma_{ph} = ne\mu = \left(\frac{\phi\alpha I\tau}{h\nu}\right) e\mu \quad (1)$$

where n is the density of carriers, e the elementary charge, μ the mobility, ϕ the charge generation quantum efficiency, α the absorption coefficient, I the optical intensity, τ the life time of charier, and $h\nu$ is the energy of photon. The photocharge generation efficiency and the hole mobility are the key parameter.

In this study, we evaluate the applied electric field-dependences of the photocurrent of the PSX-DCZ:C_{60} = 69:1, PSX-TPD:C_{60} = 69:1, and PVK:C_{60} = 69:1 mixtures. The conductivities were measured by using a conventional DC technique. DC conductivity measurements were conducted at wavelength of 633 nm. The photoconductivity was calculated as the difference between total current in the presence of light and the dark current. The measured photocurrent as a function of the external electric field is shown in Fig. 2 We can see that find figure out the photocurrents exhibited a strong electric field dependence; as the external field was increased, the photocurrent response increased. These values were found to be *ca*. 3280 nA for **PSX-DCZ**/C_{60}, *ca*. 3400 nA for **PSX-TPD**/C_{60}, and *ca*. 2224 nA for PVK/C_{60} at 60 V/μm. This nonlinear dependence on the electric field is due to the electric field dependencies of both the quantum efficiency and the charge mobility.

Table 2
Optical and electrochemical properties of the polysiloxanes

Polymer	λ_{max} (nm)[a]	Band gap (eV)[b]	HOMO (eV)[c]	LUMO (eV)[d]
PSX-DCZ	304, *sh*.349	3.23	−5.87	−2.64
PSX-TPD	304, 348	3.03	−5.49	−2.46

[a] Maximum wavelength of absorption in THF.
[b] Calculated from the absorption edge of the UV–vis spectrum.
[c] HOMO energy level was calculated by using ferrocence value of 4.8 eV below the vacuum level.
[d] Estimated from the HOMO and band gap.

As can be seen in Fig. 2 and Table 2, the photocurrent of **PSX-DCZ**/C_{60} and **PSX-TPD**/C_{60} mixture is larger than that of the PVK/C_{60} mixture. Therefore, the lower HOMO levels of **PSX-DCZ**/C_{60} and **PSX-TPD**/C_{60}, compared with the PVK/C_{60}, may lead to larger photoconductivity, which is consistent with our experiment results.

One important parameter for characterizing photoconductive material is their photogeneration efficiency. The xerographic discharge technique was used for the photogeneration efficiency at wavelength of 633 nm [11]. All the trends we are applicable for **PSX-DCZ**/C_{60}, **PSX-TPD**/C_{60}, and PVK/C_{60} mixtures in the studied electric field range of $E = 10$–60 V/μm (Fig. 3). In these results, the photogeneration efficiency of **PSX-DCZ**/C_{60} and **PSX-TPD**/C_{60} was much higher than that of the PVK/C_{60} under the same conditions. From these results, the quantum efficiency of the charge generation of **PSX-DCZ**/C_{60} and **PSX-TPD**/C_{60} was calculated to be 25.2×10^{-5} and 31.1×10^{-5} under field strength of 60 V/μm, respectively. The quantum efficiency of **PSX-DCZ**/C_{60} and **PSX-TPD**/C_{60} mixture is higher than that for the PVK/C_{60}. This is apparently due to the larger systems of conjugated π-electrons in **PSX-DCZ** and **PSX-TPD**. **PSX-DCZ**, with a longer alkyl substituent, exhibits a little lower quantum efficiency than that of **PSX-TPD**, apparently due to the lower concentration of the functional units. The quantum efficiency showed the electric field dependence which can be simulated theoretically by Onsager's model of the geminate-pair dissociation.

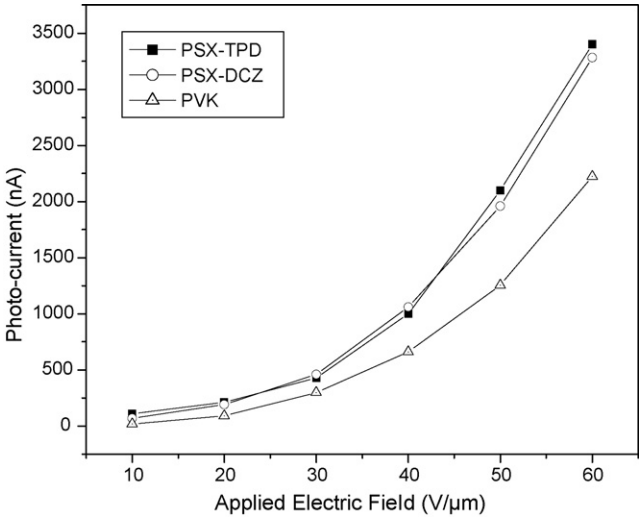

Fig. 2. Photoconductivity of the PSX-DCZ/C_{60}, PSX-TPD/C_{60}, and PVK/C_{60} as a function of external electric field strength.

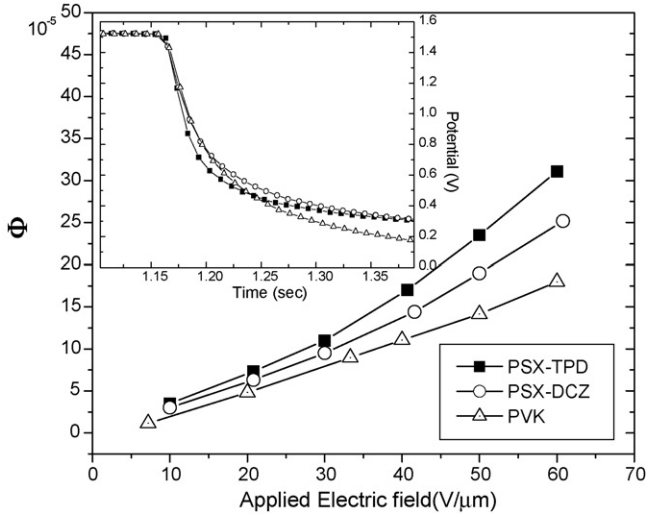

Fig. 3. Photogeneration efficiency of the PSX-DCZ/C_{60}, PSX-TPD/C_{60}, and PVK/C_{60} at various applied field. The inset shows the light-decay curves of single-layered photoreceptors for C_{60}-doped composites.

4. Conclusions

The polymers **PSX-DCZ** and **PSX-TPD** were synthesized and investigated in view of the photoconductivity of these polymers mixtures with C_{60}. **PSX-DCZ**/C_{60} and **PSX-TPD**/C_{60} are larger than that of the PVK/C_{60} mixture. This is apparently due to the larger systems of conjugated π-electrons. **PSX-DCZ** and **PSX-TPD** have better charge transporting ability than the PVK, suggesting that the polymer can be used as a hole-transporting material in various applications such as hole-transporting materials, solar cells, and photorefractive materials.

Acknowledgement

The authors acknowledge the financial support from the Ministry of Science and Technology of Korea through the Creative Research Initiatives program.

References

[1] J.V. Grazulevicius, P. Strohriegle, J. Pielichowski, K. Pielichowski, Prog. Polym. Sci. 28 (2003) 1297.
[2] H. Rost, H. Hörhold, W. Kreuder, H. Spreitzer, Proc. SPIE 3148 (1997) 373.

[4] R. Lygaitis, J.V. Grazulevicius, F. Tran-Van, C. Chevrot, V. Jankauskas, D. Jankunaite, J. Photochem. Photobiol. A: Chem. 181 (2006) 67.
[5] Y. Li, Y. Wu, B.S. Ong, Macromlecules 39 (2006) 6521.
[6] F. Goubard, R. Aîch, F. Tran-Van, A. Michalevicitue, F. Wünsch, M. Kunst, J. Grazulevicius, B. Ratier, C. Chevrot, Proc. Estonian Acad. Sci. Eng. 12 (2006) 96.
[7] O. Ostroverkhova, W.E. Moerner, Chem. Rev. 104 (2004) 3267.
[9] M. Stolka, J. Yanus, D.M. Pai, J. Phys. Chem. 88 (1984) 4707.
[10] Y. Zhang, T. Wada, L. Wang, H. Sasabe, Chem. Mater. 9 (1997) 2798.
[11] M. Umeda, T. Niimi, M. Hashimoto, Jpn. J. Appl. Phys. 29 (1990) 2746.